7.3 RECENT RESEARCH ON METEOROLOGICAL OBSERVATIONS AND INSTRUMENTATION AT KNMI

Hannelore I. Bloemink*, M.J. de Haij and W.M.F. Wauben
Royal Netherlands Meteorological Institute (KNMI), De Bilt, The Netherlands

1. INTRODUCTION

Being the National Meteorological Service of The Netherlands, KNMI operates the national meteorological observing network. This network consists of about 30 land-based Automatic Weather Stations and 10 marine-based AWS's (on North Sea oil production platforms). Also, the observations at the Dutch airports (including Amsterdam Airport Schiphol and the Air Force) are the responsibility of KNMI. Furthermore, KNMI cooperates with the ministry of Transport, Public Works and Water Management regarding the meteorological observations along the coast and the major motorways. In order to continually improve the quality of these observations and to keep them up-to-date and efficient, research into new observation techniques and improvement of existing ones is an ongoing topic.

As examples, three research topics are discussed here: improvement of cloud (cover) observations, a standard for visibility measurements and improvement of precipitation type detection.

2. CLOUD (COVER) OBSERVATIONS

Cloud observations are generally performed by human observers. KNMI uses ceilometers in combination with an algorithm to generate automated cloud reports. Since November 2002 all synoptic cloud reports in the Netherlands are generated automatically. More recently, the aeronautical cloud observations at regional airports have also been automated. Automated cloud observations are generated at about 30 locations in the meteorological network and are centrally available every 10 minutes. Currently KNMI employs human observers only at the international airports of Amsterdam and Rotterdam.

Comparisons of automated and manual cloud reports have been published before (cf. e.g. Wauben (2002) and Wauben et al. (2006)). Although the characteristic of automated and manual cloud observations are different the synoptical users have accepted the automated cloud observations. Advantages of the automated cloud observations are they are subjective, consistent, and have a higher spatial density and temporal resolution that the manual observations. However, the large differences that can occur in certain situations are a concern for specific applications.

Figure 1: NubiScope at Cabauw.

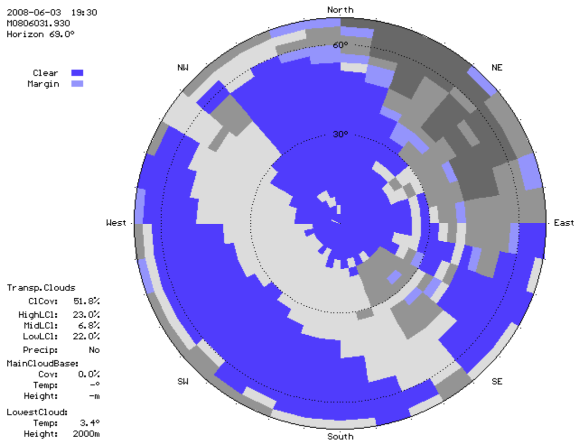

Figure 2: The sky at Cabauw on 30 June 2008 19:30 UT as observed by the NubiScope. Shown is a cloud mask in a colour scheme that simulates a visual observation.

A limitation of the automated cloud observations by ceilometers is the lack of spatial representativeness. For that purpose KNMI purchased a so-called NubiScope in order to evaluate it's usefulness for cloud observations.

* *Corresponding author address*: Hannelore Bloemink, Royal Netherlands Meteorological Institute (KNMI), Instrument R&D section, P.O. Box 201, 3730 AE, De Bilt, The Netherlands; email: bloemink@knmi.nl

The NubiScope (cf. Figure 1) consists of a pyrometer sensitive in the thermal infrared (10-14µm) with a field of view of 3° mounted on a pan-and-tilt unit. The NubiScope works fully automated and performs a scan of the overhead hemisphere (36 azimuth and 30 zenith angles) and 2 surface temperature measurements every 10 minutes. Details of the NubiScope are given in Wauben (2006). The observed temperatures are processed in order to derive the obscuration type (fog, precipitation, clouds) and cloud characteristics (cloud cover, layering and altitude). The NubiScope determines the presence of clouds from the deviation of the measured sky temperature for a clear sky value. The cloud height follows from the temperature by assuming a standard temperature profile where the temperature observed at the horizon serves as the ambient temperature. This, in combination with other factors such as the absolute calibration and contamination of the pyrometer as well as the possibility of mixed scenes in the field of view or the presence of semi-transparent clouds, makes the height information rather uncertain. It might by improved by considering information obtained from other sensors, but here only cloud cover considered. Figure 2 shows a cloud mask generated by the NubiScope that shows the spatial distribution of low, middle and high clouds.

The NubiScope has been installed at the Cabauw research site of KNMI since April 2008. The cloud observations have been compared against the automated cloud reports generated by a Vaisala LD40 ceilometer as well as with other instruments such as LIDAR, cloud radar, visual sky camera (TSI). The total cloud cover results of the NubiScope and the LD40 are given in a contingency table in Table 1. The green diagonal contains 47% of the data where LD40 and NubiScope give identical total cloud cover. The yellow and orange bands contain 82% and 90% of the data that is within ±1 and ±2 okta, respectively. The averaged difference in total cloud cover is 0.07 okta and mean absolute deviation is 1.0 okta. The differences between the NubiScope and the LD40 are similar to the differences observed between the manual observer and the LD40. As a result of scanning the NubiScope is able to detect clouds in almost clear sky situations or gaps in overcast situations. This is illustrated by the reduced number of occurrences of 0 and 8 okta for the NubiScope compared to the LD40.

Further evaluations have been performed by observers at Rotterdam airport (30km distance) with access to the 10-minute sensor data. For 2 months evaluations have been performed when the differences between NubiScope and LD40 exceeded 2 okta. Their findings have been entered in a web tool (cf. Figure 3). The evaluation showed that the observed differences could mostly be attributed to the better spatial representativeness of the NubiScope compared to the LD40. Furthermore, the sensitivity of the NubiScope for high clouds is often better than that of the LD40, but certainly not as good as that of the cloud radar.

The Climate department decided to keep the NubiScope as a permanent instrument at the Cabauw research site. The Weather department confirmed the added value of the NubiScope for cloud cover observations, but for applications such as aviation the cloud height information is crucial. Hence the cloud information obtained by the NubiScope cannot be used unless accurate height information is also available.

LD40 AUTOSYNOP (okta)	NubiScope (okta)										
	NA	0	1	2	3	4	5	6	7	8	Sum
NA	165	431	439	122	101	101	91	94	722	779	3045
0	1234	2515	1958	167	74	53	40	40	142	58	6281
1	1136	2074	2155	440	180	119	99	74	312	188	6777
2	342	432	630	276	181	88	62	39	176	110	2336
3	331	182	370	276	238	129	83	56	258	105	2028
4	381	64	228	229	237	188	138	86	324	92	1967
5	423	31	117	134	189	213	193	174	441	127	2042
6	474	11	59	71	128	201	228	227	729	228	2356
7	1704	12	44	31	74	180	381	657	3401	2138	8622
8	3359	13	38	12	10	21	39	136	3931	9547	17106
Sum	5765	6038	1758	1412	1293	1354	1583	10436	13372	5765	52560

Δn±0 = 47% Δn±1 = 82% Δn±2 = 90% <Δn> = 0.07 <|Δn|> = 0.95

Table 1: Contingency table of the 10-minute total cloud cover reported by NubiScope versus LD40 for the period May 2008 – May 2009 in Cabauw.

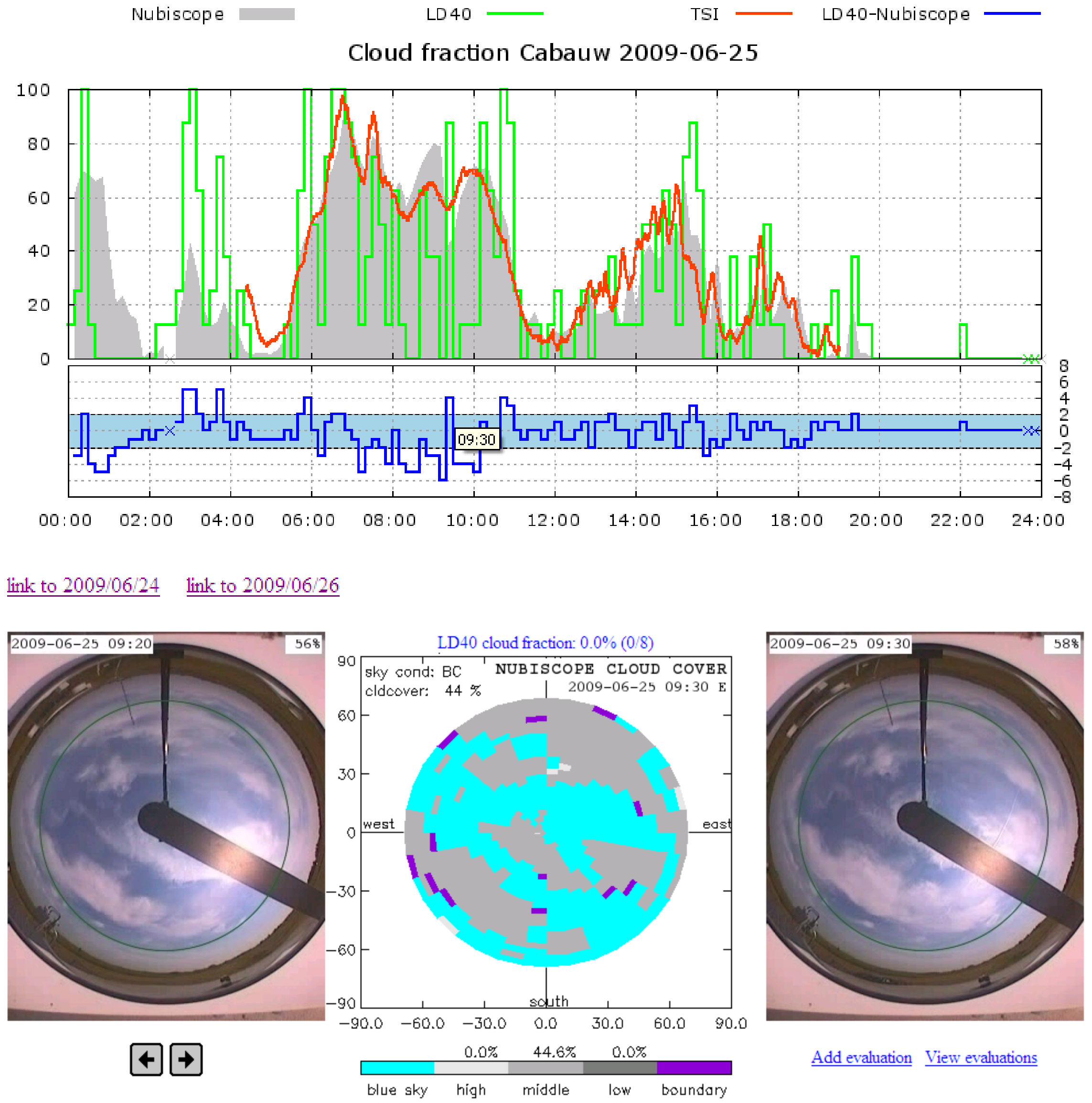

Figure 3: The NubiScope evaluation screen showing: a daily overview of the total cloud cover of NubiScope (gray), LD40 (green) and TSI (red) on June 25th, 2009 and the differences LD40-NubiScope (blue) (top); the video images of the TSI at the start and end of the NubiScope scan and the NubiScope cloud mask at 9:30UT (bottom).

3. VISIBILITY STANDARD

Scatterometers (or forward scatter sensors) are used to measure visibility. Calibration of scatterometers is not trivial. When scatterometers are used for aeronautical purposes, their calibration needs to be traceable and verifiable to a transmissometer standard, the accuracy of which has been verified over the intended operational range (see ICAO, 2004). The KNMI visibility standard consists of a calibrated transmissometer and a scatterometer and is operated in De Bilt. The result is a calibration device which can be used to calibrate FD12P scatterometers, in accordance with the above regulations. The standard also allows regular checks of this calibration device, as well as a check of the linearity of the scatterometer.

3.1 *Calibration chain*

The calibration chain of the scatterometers used by KNMI, the Vaisala FD12P Present Weather Sensor, is shown schematically in Figure 4.

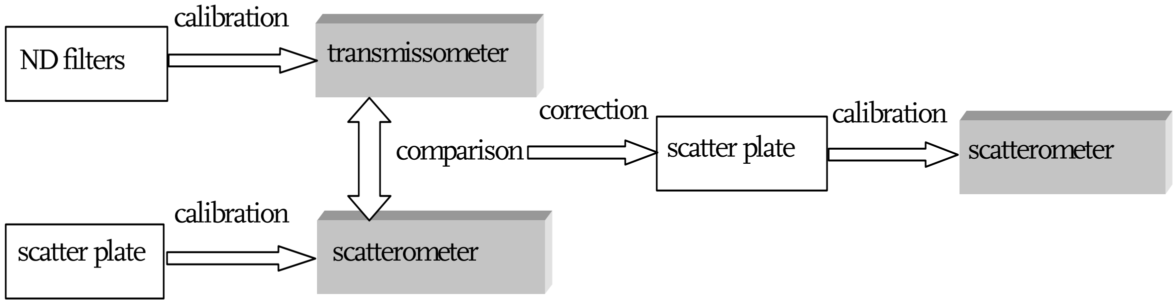

Figure 4: The visibility standard shown schematically. See text for explanation.

Transmissometer calibration

The calibration chain for the FD12P scatterometer starts with the calibration of a transmissometer. Transmissometers are calibrated (and adjusted) using Neutral Density Filters. These filters are in turn calibrated in the laboratory and are thus the primary source of calibration in the chain. The ND filters are placed in the baseline of the instrument and the transmission is measured by the instrument. Several filters are used with transmissions of approximately 0.25, 0.4, 0.6 and 0.8. Combination of these filters will provide additional data points. Comparing the measured transmission with the filter transmission will give the deviation from linearity of the instrument, which can be corrected for by the software.

Initial scatterometer calibration

Initially, the FD12P scatterometer of the standard is calibrated in the usual way. This means a calibration device called “scatter plate” is placed in the measuring volume of the instrument and the instrument is adjusted accordingly. More details can be found in instrument’s manual (see Vaisala (2002)).

Comparison between transmissometer and scatterometer

An important part of the visibility standard is the comparison of the transmissometer and scatterometer in the standard. The two instruments are installed in the field close to each other, and the data are collected continuously (for details, see the measurements section of this paper). The Meteorological Optical Range (or MOR) values of the two instruments are compared, as this quantity depends solely on the state of the atmosphere and not on parameters like background luminance and lamp settings. The results of this comparison will indicate if the scatterometer agrees with the transmissometer within the required accuracy, or if the scatterometer needs to be adjusted. The amount of data used needs to be sufficient to make a good comparison. In practice for the setup in De Bilt, this can vary from 2 months to 6 months.

Adjustment of the scatter plate

The previous step may indicate that the scatterometer of the standard deviates too much from the transmissometer and an adjustment is needed. For the FD12P, this can be achieved by adjusting the scatter plate, a device used for calibration of the FD12P. This is a glass plate which can be inserted into the measuring volume, resulting in a known amount of scatter. This amount is then input into the software of the instrument, and the instrument is adjusted. The value corresponding to this amount of scatter is adjusted such, that the FD12P visibility corresponds to the transmissometer visibility.

Calibrating other scatterometers

The previous step has resulted in a scatter plate which is now well calibrated and can be traced back to a transmissometer standard. So this scatter plate can now be used to calibrate/adjust other FD12P’s. This means that it is not necessary to place the instruments in the standard. They can be calibrated in the field or in the laboratory using only the scatter plate.

So the final result of the calibration chain is a well calibrated scatter plate which is used to calibrate FD12P’s.

3.2 *Measurements*

The two instruments used in the visibility standard are the Vaisala transmissometer Mitras and the Vaisala scatterometer FD12P Present Weather Sensor. Both instruments have a measuring height of 2.5 m, in accordance with airport regulations for visibility measurements. The FD12P is placed at roughly the centre of the long baseline of the Mitras.

The Mitras transmissometer used is a double baseline system. In the chosen setup, the range of the instrument is 8 m – 3 km. The Vaisala FD12P uses IR light at 875 nm, which is detected under an angle of about 30°. The amount of scatter measured in this way is empirically linked to the extinction coefficient.

In order to compare the two instruments of the standard, the data need to be filtered properly. Details of this filtering process can be found in Bloemink (2006). The main issue is that the visibility needs to be stable in order to compare the instruments properly. This is ensured (according to ICAO recommendations, see ICAO (2000)) by determining the average and standard deviation of the measured MOR values within a 10-minute interval. If the standard deviation is larger than 10 % of the average, then the interval is not used.

3.3 *Results*

The results of the comparison of the two instruments are shown in Figure 5 for 12 months of data, from September 2005 to August 2006. Explanations of the Figure can be found in the caption.

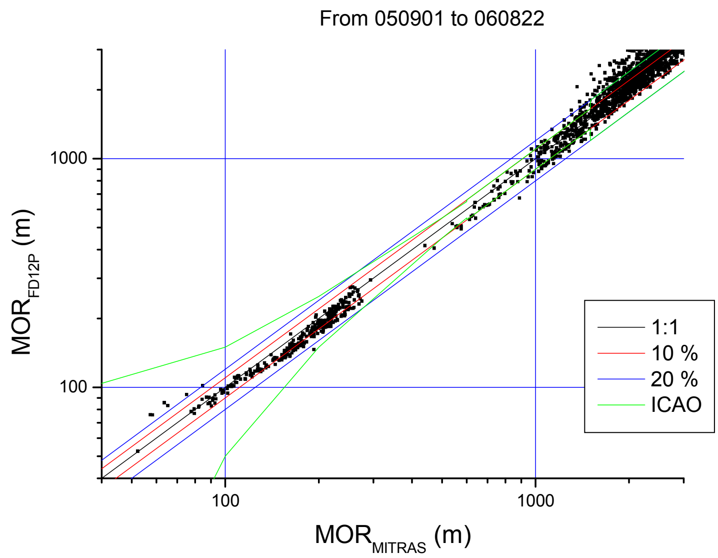

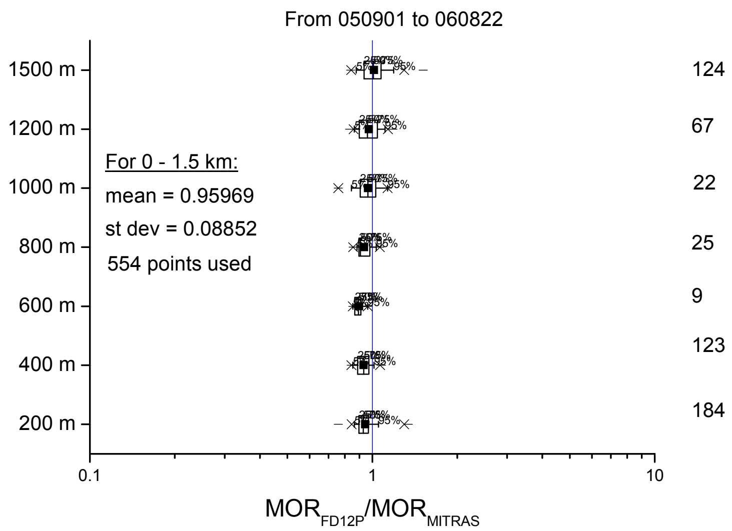

Figure 5: Upper panel: 10 minute averages of the MOR from the FD12P (y-axis) as a function of the MOR from the Mitras (x-axis) for the 12 months of data indicated. Also shown are the ICAO limits (green line), the 20 % difference lines (blue), 10 % difference

lines (red) and the 1:1 line (black). The applied data filtering is described in the text. Lower panel: The same results as a box plot. On the x-axis the ratio MOR_{FD12P}/MOR_{Mitras}. On the y-axis, 200 m means MOR_{Mitras} between 0 and 200 m, 400 m means MOR_{Mitras} between 200 and 400 m, etc... On the right the number of data point are indicated. The percentages for the box plot are: box: 25 - 75 %, I: 5 - 95%, ×: 1 – 99 % and -: minimum and maximum.

For these data, the mean of the ratio MOR_{FD12P}/MOR_{Mitras} is 0.96, with a standard deviation of 0.09. The distribution of the visibilities is indicated of the right-hand side of Figure 5 where the numbers are the number of data points for the interval indicated on the y-axis.

An uncertainty analysis of the visibility standard naturally follows the scheme shown in Figure 4. Details can be found in Bloemink (2006).

3.3 *Discussion and conclusion*

The first thing that is evident from the results, is that there is not a lot of data available for a good comparison. In total, there are only 554 10-minute averages available for about 1 year of continuous measurements. The main reason for this is that only stable visibility conditions can be used to compare the two instruments, and the requirements for these conditions are very strict (see Measurements section). This is the reason why a good comparison may take a relatively long time. This naturally depends also on the climate at the location of the standard.

Another thing that shows clearly in Figure 5, is that there is very little data between about 300 and 800 m. This is also a result of the fog conditions at the location of the standard. Fog with these visibilities is usually fog that is forming or dissipating, and thus it is not very stable. This can obviously not be helped, but as long as there are enough data points on either side of this interval, the data can be used for the standard.

The main result from the comparison of the instruments is that the mean of the ratio MOR_{FD12P}/MOR_{Mitras} is 0.96, with a standard deviation of 0.09. This means that within the margin of error, the instruments agree with one another. So the scatter plate does not need adjusting, and can be used to calibrate other FD12Ps. Checks like these can be used on a regular basis (*e.g.* once a month) to check the scatter plate and instruments for degradation effects.

Both plots of Figure 5 give information on the linearity of the scatterometer. Around roughly 200 m, the FD12P gives somewhat lower visibilities, but the differences are of about the same order as the standard deviation. Around 100 m and 1000 m both instruments agree very well.

In conclusion, the visibility standard of KNMI can be used to calibrate FD12P scatterometers. The standard ensures that the calibration can be traced back to a well-defined transmissometer standard, in accord with civil aviation regulations. A regular check of the calibration device used for the FD12P scatterometers is also part of the standard, as is a check of the linearity of the FD12P.

4. PRECIPITATION TYPE DETECTION

KNMI operates the Vaisala FD12P present weather sensor for observations of visibility, precipitation type and duration in the national meteorological observation network. The sensor uses the principle of forward scattering of infrared light in a small volume of air. Precipitation type is derived internally by analysing the signals from the optical receiver and a capacitive rain detector, together with temperature. However, some shortcomings of this observation have been recognized since its introduction (e.g. Wauben (2002), Van der Meulen (2003)), particularly with precipitation type discrimination around zero degree Celsius, hail detection and the detection of very light precipitation events.

Although correction algorithms were introduced and further research into the use of raw data from the present weather sensor was executed (see Bloemink (2004)), it was concluded that an improvement for the mixture of rain and snow was not likely (see De Haij (2007)). Therefore, it was decided to investigate the performance of new sensors for the observation of precipitation type, and investigate their added value over the FD12P.

4.1 *Instruments*

Four commercially available sensors were selected and purchased for this test in the beginning of 2008. The Thies Laser Precipitation Monitor (LPM) and Ott Parsivel are so-called optical disdrometers that measure the extinction in a horizontal sheet of light to estimate the diameter and fall velocity of each individual particle. Whenever a particle falls through the sample area the signal voltage at the receiver side is reduced. The particle size can be derived from the amplitude of the signal drop, whereas the duration determines the fall velocity of the particle.

The LPM operates at 785 nm and has a sample area of 46 cm^2. Beside precipitation intensity and amount, the output comprises drop size distribution (0.16-7 mm), fall velocity (0.2-20 m/s) and precipitation type (P, L, LR, R, LRS, S, SG, SP, A) in several code types (see Table A). Precipitation is automatically classified as liquid when the measured temperature is above 9 ºC (except hail) and as solid below -4 ºC. The Parsivel (wavelength 650 nm and sample area 54 cm^2) also reports the drop size distribution (0.2-25 mm) and fall velocity (0.2-20 m/s) and is able to discriminate between a large number of precipitation types (L, LR, R, LRS, S, SG, SP, A).

Also included in the test is the Lufft R2S-UMB sensor, a small 24 GHz Doppler radar system that measures the fall speed of hydrometeors falling in a cone above the sensor dome. The precipitation quantity is calculated by means of the correlation of raindrop size and speed. The sensor reports precipitation type (R, LRS, S, A), precipitation quantity and ambient temperature. The R2S is mainly used in road weather applications.

Precipitation type	PW code	NWS code	METAR code
No precipitation	00	C	-
Unknown precipitation	40	P	UP
Drizzle	50	L	DZ
Freezing drizzle	55	ZL	FZDZ
Drizzle and rain	57	LR	DZRA
Rain	60	R	RA
Freezing rain	65	ZR	FZRA
Drizzle/rain and snow	67	LRS	RASN
Snow	70	S	SN
Ice pellets	75	IP	PL
Snow grains	77	SG	SG
Ice crystals	78	IC	IC
Snow pellets	87	SP	GS
Hail	89	A	GR

Table 2. Overview of the different precipitation types of interest in this study, and the corresponding PW, NWS and METAR codes.

The Vaisala WXT520 weather transmitter is an all-in-one compact weather station for pressure, temperature, humidity, wind and precipitation amount. The voltage output from the piezoelectric detector due to a drop impact is proportional to the drop size. The WXT520 is able to distinguish between rain and hail particles by analysing the characteristics of the individual drop impact signals. The sensitivity threshold for the detection of a single droplet is estimated on a diameter of about 0.8 mm.

4.2 *Field test and evaluation*

The sensors are installed on the test field in De Bilt since 12 September 2008 (see Figure 6. The sensors are collocated within 30 m of the FD12P and the other meteorological sensors, which offers the opportunity to analyse the relation with other parameters (e.g. precipitation amount, wind) as well. All sensors are installed at 1.5 m above the surface, except for the Lufft R2S (2m). The sample areas of the LNM and Parsivel sensors are oriented perpendicular to the prevailing south-westerly wind direction with precipitation in De Bilt. Except for the removal of spider webs on some occasions, no maintenance was carried out on the sensors.

Figure 6: The test field in De Bilt, with the four precipitation type sensors under test indicated in the foreground.

Data messages are acquired every minute and averaged to 10-minute and hourly weather codes, which are evaluated on a routine basis by data validation specialists and meteorologists. They enter their level of agreement with the sensors in a web-based form.

A winter situation where the Thies LPM and Ott Parsivel significantly deviate from the FD12P is presented in Figure 7. Both optical disdrometers start to report mixed and solid precipitation from 16UT, which is in better agreement with the evaluation of the meteorologist than the rain reported by the FD12P. The reported large amount of hail reports by the Parsivel, which is a common feature for this sensor, has however not been confirmed. Note furthermore that the LPM seems more sensitive for very light precipitation, reporting a significant number of drizzle events between 13 and 14UT. The detection and precipitation type capabilities of the Lufft R2S and Vaisala WXT520 seem inadequate.

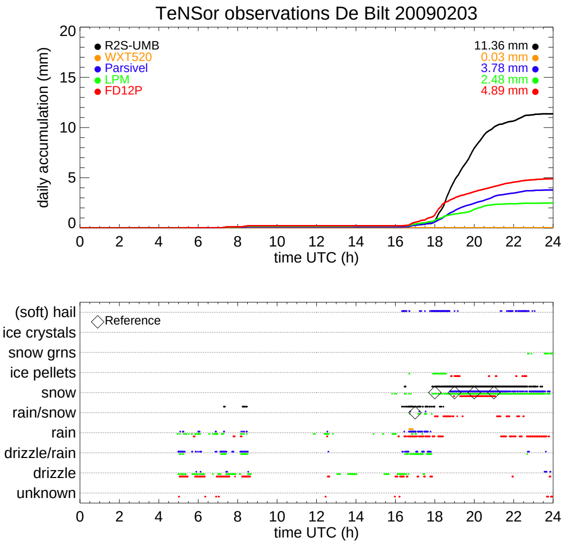

Figure 7. Precipitation accumulation and precipitation type measured in De Bilt on 3 February 2009. The reported precipitation types are shown in the lower panel, with the observation of the meteorologist ('Reference') indicated by black diamonds.

Another case, where the FD12P falsely detects precipitation during dense fog, is illustrated in Figure 8. Visibility values drop below 200 m shortly after 21UT, leading to successive precipitation reports in the form of snow and snow grains with intensities up to 0.03 mm/h. Improvement can be achieved on this point as well, as the other sensors in the test clearly suffer less from this problem.

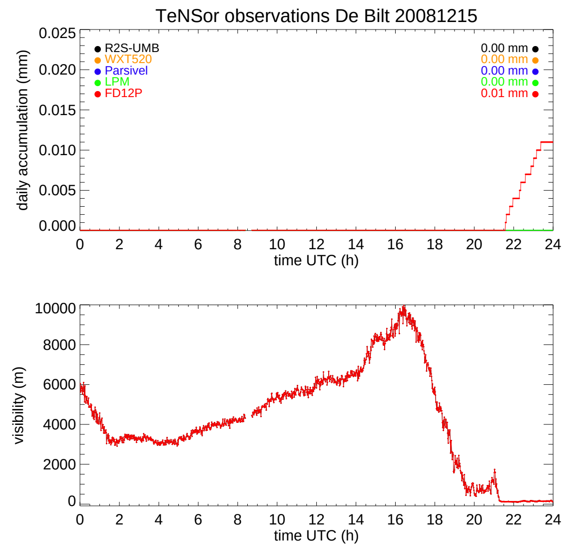

Figure 8. Precipitation accumulation and visibility (MOR) measured in De Bilt on 15 December 2008. The first faulty detections by the FD12P in dense fog are seen just before 22UT.

4.3 *Conclusions*

Based on the evaluation in the first winter of the test, the Thies disdrometer is the most promising sensor that could improve the precipitation type and detection observation in the observation network of KNMI. More specifically, it seems to give added value on hail discrimination and demonstrates good results during transitions between liquid and solid precipitation and the detection of very light precipitation. It should however be mentioned that the Thies disdrometer also has its shortcomings, i.e. it suffers from false detections due to insects and spider webs and shows a significant wind direction dependency of the measured precipitation amount. The latter was confirmed in e.g. Upton and Brawn (2008) and an analysis of data from three LPM sensors of the German Weather Service (DWD) with different orientations.

4.4 *Outlook*

Wintry precipitation events in one season are sparse and the evaluation by meteorologists has its limitations, because the meteorologist scarcely has the opportunity to perform a detailed evaluation during solid precipitation events. Therefore the test is continued in the winter season 2009-2010.

Furthermore a second field test with the LPM at an airport is being considered since the human observer can play an important role in the evaluation. In addition, the combination of the results of the rain gauge, the FD12P and the disdrometer in order to obtain an optimal precipitation detection and type discrimination needs to be investigated in more detail.

5. REFERENCES

Bloemink, H.I., 2004: Precipitation type detection Present Weather Sensor. Final report. KNMI Technical Report No. 259, KNMI, De Bilt, The Netherlands.

Bloemink, H.I., 2006: KNMI Visibility standard for calibration of scatterometers, Paper presented at the WMO Technical Conference on Instruments and Methods of Observation (TECO-2006), Geneva, Switzerland, 4 – 6 December 2006, IOM 94 (TD1354).

Haij, M.J. de, 2007: Automated discrimination of precipitation type using the FD12P present weather sensor: evaluation and opportunities. KNMI Technical Report No. 297, KNMI, De Bilt, The Netherlands.

ICAO, 2000: Manual of Runway Visual Range Observing and reporting practices, Doc. 9328-AN/908. 2nd edition, ICAO.

ICAO, 2004: Annex to the Convention on International Civil Aviation; Meteorological Service for International Air Navigation, 15th edition, July 2004, chapter 4.3: runway visual range.

Meulen, J.P. van der, 2003: Exploratory actions on automatic present weather observations. Final report. EUMETNET PWS-SCI report, De Bilt, The Netherlands.

Upton, G. and D. Brawn, 2008: An investigation of factors affecting the accuracy of Thies disdrometers. Paper presented at the WMO Technical Conference on Instruments and Methods of Observation (TECO-2008), St. Petersburg, Russian Federation, 27-29 November 2008, IOM 96 (TD1462).

Vaisala, 2002: User's Guide Weather Sensor FD12P, M210296en-A, May 2002, Vaisala.

Wauben, W.M.F., 2002: Automation of visual observations at KNMI; (I) Comparison of present weather. Paper presented at the Symposium on Observations, Data Assimilation, and Probabilistic Prediction, Orlando, Florida, 13-17 January 2002, American Meteorological Society.

Wauben, W.M.F., 2006: Evaluation of the NubiScope. KNMI Technical Report TR 291, De Bilt, the Netherlands.

Wauben W., H. Klein Baltink, M. de Haij, N. Maat and H. The, 2006: Status, Evaluation and New Developments of the Automated Cloud Observations in the Netherlands. Technical Conference, 4-6 December 2006, IOM-94, TD-1354, WMO, Geneva, Switzerland.